

Feature extraction and gait classification in hip replacement patients on the basis of kinematic waveform data

Carlo Dindorf¹, Wolfgang Teuffl², Bertram Taetz³, Stephan Becker¹, Gabriele Bleser⁴, Michael Fröhlich¹

¹ Department of Sports Science, Technische Universität Kaiserslautern, Kaiserslautern, Germany; ² IFFB Sport and Movement Science, Paris Lodron University Salzburg, Austria; ³ Department Augmented Vision, German Research Center for Artificial Intelligence (DFKI), Kaiserslautern, Germany; ⁴ Junior Research Group wearHEALTH, Technische Universität Kaiserslautern, Kaiserslautern, Germany

Abstract

Study aim: To find out, without relying on gait-specific assumptions or prior knowledge, which parameters are most important for the description of asymmetrical gait in patients after total hip arthroplasty (THA).

Material and methods: The gait of 22 patients after THA was recorded using an optical motion capture system. The waveform data of the marker positions, velocities, and accelerations, as well as joint and segment angles, were used as initial features. The random forest (RF) and minimum-redundancy maximum-relevance (mRMR) algorithms were chosen for feature selection. The results were compared with those obtained from the use of different dimensionality reduction methods.

Results: Hip movement in the sagittal plane, knee kinematics in the frontal and sagittal planes, marker position data of the anterior and posterior superior iliac spine, and acceleration data for markers placed at the proximal end of the fibula are highly important for classification (accuracy: 91.09%). With feature selection, better results were obtained compared to dimensionality reduction.

Conclusion: The proposed approaches can be used to identify and individually address abnormal gait patterns during the rehabilitation process via waveform data. The results indicate that position and acceleration data also provide significant information for this task.

Keywords: Classification – Total hip arthroplasty – Feature selection – Dimensionality reduction

Introduction

The total hip arthroplasty (THA) is the most important surgery for the treatment of degenerative hip osteoarthritis [26]. Postoperative changes in gait can not only affect the operated joint and the surrounding structures, but also influence the contralateral side. In addition, postoperative gait patterns often display an asymmetric character [2, 17]. The possible consequences include increased joint loadings, which could lead to injuries and a failure of the implant, resulting in the need for further surgical interventions [21].

Gait classification is an important tool for clinical diagnostic and illness identification [13, 14]. The classification of the operated hip side could deliver knowledge about the best discriminative variables and is, therefore, of

clinical relevance. With modern movement tracking systems, a huge amount of data are available (big data) [30], and machine learning models have gained importance compared to classical statistical approaches [6]. Feature selection and dimensionality reduction are important steps toward improving a model's accuracy and interpretability, preventing overfitting, and reducing the necessary computing power [25].

Joint angles at specific points in time and descriptive statistics, such as the total range of motion or peak values, are commonly used for classification [3]. However, it is questionable whether such features optimally map group differences or if meaningful information is discarded a priori. For example, acceleration data have been given relatively little consideration, although it has been shown that they map important information about gait patterns [16]. The dependence on prior knowledge, assumptions,

or subjective decisions is a further limitation. The use of entire gait waveforms that have been transformed using principal component analysis (PCA) could be a potential alternative [13, 30]. Comparative studies regarding different dimensionality reduction methods and classification algorithms have rarely been reported [14]. To the best of our knowledge, the use of feature selection on gait waveform data and classification in the context of THA (for classification of THA patients and healthy subjects, see [12, 34]) has hardly been investigated so far. Therefore, this work applies feature selection to gait waveform data of THA patients to objectively deduce discriminative variables (including discriminative time points in a gait cycle), which are most important for the description of asymmetrical gait. In order to do this, patients are classified according to the operation side after unilateral THA. The classification results were compared with those obtained through the use of different dimensionality reduction methods for feature extraction.

Materials and methods

Subjects and data acquisition

Motion data were collected from 22 subjects (P1–P22; 7 males, 15 females; age: 56.90 ± 8.20 ; height: 1.74 ± 0.08 ; weight: 82.90 ± 18.85) after THA (11 left side, 11 right side). The adequate sample size was derived from previous gait classification studies [3, 10]. All subjects were recruited from among patients of the Klinik Lindenplatz (Bad Sassendorf, NRW, Germany). All measurements were conducted in the biomechanics laboratory of the institute of biomechanics of the Klinik Lindenplatz.

Patients were only considered fit to participate in the study if they were at least 14 days, but not more than 21 days, after surgery. The subjects had to be able to walk steadily for at least six minutes without support on even ground to be included in the examination. All included patients received a standard cemented THA using a direct anterior or lateral approach [36]. The patients were allowed to bear their full weight by their attending physicians at the time of measurement.

After receiving all relevant study information, the patients signed an a form indicating their informed consent to the study, which included permission to publish the data. The study was approved by the responsible ethics commission and meets the criteria of the Declaration of Helsinki.

The gait data of the lower bodies of the THA patients were recorded during a 6 minute walking test using an OptiTrack® stereophotogrammetric motion capture system (NaturalPoint, Inc., Oregon, USA). The accuracy of the OptiTrack motion capture system was shown in recent publications [9, 35].

The subjects were equipped with retroreflective markers attached to anatomical landmarks according to the recommendations of Leardini et al. [23]. For hygienic reasons, the subjects had to wear shoes. Therefore, the markers corresponding to the foot had to be positioned on the surface of the shoe, approximating the underlying anatomical landmarks. The 3D positions of the markers during movement were recorded with a frame rate of 60 Hz. The walking direction was along the x-axis according to the defined global coordinate system, with the z-axis drawn vertically.

Data preparation

The following steps described below were performed separately for each subject: In addition to marker position data, the marker velocity and acceleration, as well as joint and segment angles, were calculated to check if those variables have higher importance. Missing data points were interpolated using spline interpolation (maximum gap = 5 frames). Noise attenuation was performed using a low-pass Butterworth filter (cutoff frequency = 6 Hz). With the marker position data, the marker velocity and acceleration were calculated. The joint and segment angles were calculated using Visual3D (V6 professional, Germantown, Maryland, USA).

The turning movement at the end of the gait path as well as steps from gait initiation and stopping were removed from the data. For direct comparison of the operated and non-operated legs, the raw data were split into gait cycles for each leg separately. The beginning of a gait cycle was defined as the point of the heel marker (LCA for the left body side, RCA for the right body side; all patients started contact for both legs with the heel) with the lowest z-axis position (initial contact). Incomplete cycles were dropped. Marker trajectories were rotated so that all movements followed one direction along the x-axis. Trajectories along the y-axis were inverted for the right body side so that they fit to the trajectories of the contralateral side. The mean position for every determined cycle determined along each marker and its three axes was subtracted from the respective sequences for centering the position data and for elimination of anthropometric differences between subjects (see, e.g., [13]). Afterwards, the respective variables of each gait cycle were individually time-normalized to 101 time steps (from 0% to 100%) using cubic spline interpolation. The isolation forest algorithm was used for outlier removal. Outliers are defined as minority of all instances with very different feature values compared to normal instances. With the algorithm, the respective instances are isolated and not detected by using distance or density measurements [24]. In the current case, most of the detected outlying cycles showed very different gait patterns compared to the majority of cycles (e.g., due to visually visible compensatory movements to maintain the balance or abnormally shortened swing phases due to early contact

with the ground). Asymmetric sequences were calculated by subtracting the gait cycles (separately for each of the x, y and z movement directions of the marker trajectories, the marker velocities and accelerations as well as the joint and segment angles in each plane) of the right body side from those of the left. The corresponding sequences are denoted as a w-feature in the following. The resulting sequences were concatenated into a vector of 8,383 dimensions, where each time step maps one dimension (Table 1). The dimensions were achieved through:

- x, y and z – movement directions of the 13 markers ($3 \times 13 \times 101$ time steps = 3939);
- marker-velocities as well as – accelerations of the 13 markers ($2 \times 13 \times 101$ time steps = 2626);
- joint and segment angles in three planes of the six joint and segment angles ($3 \times 6 \times 101$ time steps = 1818).

Finally, 50 random samples (without replacement) were extracted from 70 to 120 gait cycles for every subject, resulting in a final vector with a size of $1,100 \times 8,383$ (cycles \times features), where one sample represents the

difference between the left and right side during one gait cycle.

Feature extraction and classification

Feature extraction and classification were integrated into a leave-one-group-out cross-validation (LOGO, 11 folds) process to obtain an unbiased accuracy score (test data were not used for feature extraction) and to check if classification can individual differences take into account. The basic principal behind LOGO is that for each hold-out group, model fitting is performed, using the data of all the subjects except the hold out, which is only used for model evaluation [37]. A group of two subjects was formed – one on whom the operation was on the right side, and the other on the left side. Each resulting fold consists of 1000 training samples of 20 patients and 100 test samples of 2 patients. The initial input features were independently standardized (z-transform) based on the respective training sets before application of the different extraction methods. The methods are described below.

Table 1. Initial input features. The naming convention of the markers is according to [8]

	Location/Description	Name	Type	Steps
Marker	anterior superior iliac spine	ASIS		
	posterior superior iliac spine	PSIS		
	lateral prominence of greater trochanter	GT		
	midline of the thigh	TH		
	lateral prominence of lateral femoral epicondyle	LE		
	proximal tip of the head of the fibula	HF	x-axis pos. (X)	
	anterior border tibial tuberosity	TT	y-axis pos. (Y)	
	midline of the shin	SK	z-axis pos. (Z)	
	lateral prominence of the lateral malleolus	LM	velocity (v)	
	Achilles tendon insertion	CA	acceleration (a)	
	dorsal margin of the fifth metatarsal head	VM		$\times 101$ time steps
	dorsal margin of the first metatarsal head	FM		
	distal phalanx hallux	DP1		
Joint angle	ankle angle	ANKLE_ANGLE		
	hip angle	HIP_ANGLE	flexion and extension in sagittal plane (X)	
	knee angle	KNEE_ANGLE	abduction and adduction in frontal plane (Y)	
Segment angle	foot angle	FOOT_ANGLE	axial rotation in transverse plane (Z)	
	shank angle	SHANK_ANGLE		
	thigh angle	THIGH_ANGLE		

Terminology: Feature labels are composed of marker/joint name _ type _ frame number, e.g., VM_a_46

Two different ranking approaches were applied to find relevant features for classification: a) random forest (RF) feature ranking and b) a minimum-redundancy maximum-relevance (mRMR) filter.

a) Random forest is a powerful algorithm for both regression and classification tasks. It is based on the combination of many weak learners to create one strong learner (ensemble method) [5]. The algorithm enables the calculation of a feature importance (FI) score and was applied in the following with 100 trees. Gini importance – normalized so that the total sum for all features used is one – was used as an importance score.

The following procedure was repeated until no features were left: Features were ranked with the RF algorithm according to their median feature importance based on 10 runs on bootstrap samples (80% of the dataset size). The feature with the highest importance was selected and ranked according to the time at which it was included. Afterward, features related to the selected one (a whole w-feature corresponding to the selected feature), as well as features with zero FI, were excluded. With the reduced feature set, the process was repeated. The proposed approach should be able to reduce redundancy by only selecting one point in time (the most important feature) per w-feature.

Variations in the training data often lead to different feature preferences. The robustness to these changes is described as stability [20]. Ensemble feature selection is reported as a promising approach for reducing instability [1]. The basic principal is that a combination of different feature selection processes leads to increased stability [1]. Therefore, feature ranking was performed with the proposed approach on different data samples (homogeneous feature selection) of each training fold during the LOGO process. Instead of bootstrap samples, which are commonly used for data variation, data of one group were excluded for each iteration. Due to the small number of subjects, this should lead to highly different data samples. Afterward, the different ranking lists were aggregated into one ensemble ranking. Minimum union (Min) aggregation was used to combine the ranking lists. Based on the ensemble rankings, final feature subsets were obtained with the following cut-off thresholds: 1%, 5%, 10%, 20%, 50%, and 100%.

b) The proposed RF approach does not capture redundancy between different w-features. In addition, redundancy increases through the aggregation step [32]. To obtain a mutual information-based ranking of the most relevant and minimally redundant features, an mRMR filter [28] was applied to reduce the impact of redundant features. Therefore, the features of the final ensemble list of each fold were ranked according to the mRMR filter. The classification results were then compared with the results of the proposed RF approach.

Finally, the results obtained using feature selection were compared with the following dimensionality

reduction methods: PCA, kernel PCA (kPCA), factor analysis (FA), and linear discriminant analysis (LDA). Due to the lack of comparative studies, various dimensionalities of input features and combinations with the support vector classifier (SVC) and RF were considered. Due to collinearity, PCA (99% variance threshold to select the number of components) was applied before LDA. The evaluation was performed using LOGO.

Classification algorithm and further calculations

The support vector classifier (SVC) is a commonly used algorithm for gait classification [22, 34], and was applied with a linear kernel in the current study. Stability was evaluated using the mean Jaccard similarity of the pairwise comparison between the different subsets and threshold values during the LOGO procedure (see e.g. [7]). The more similar the different subsets are, the higher the stability of the selection approach is. Calculations were made with the Python scikit-learn package (machine learning, data mining) [27].

Results

Feature selection

The classification results for the feature selection with different threshold values and the use of the SVC with a linear kernel are presented in Table 2. The best classification performance was obtained without the application of a threshold value (threshold = 100%). The corresponding subsets also showed the highest stability. Using other classification algorithms with the features of the 100% threshold also led to high classification performance (SVC with a radial basis function (rbf) kernel: $87.64 \pm 18.81\%$, $M_{AUC} = 0.96 \pm 0.07$; logistic regression: $90.45 \pm 16.78\%$, $M_{AUC} = 0.91 \pm 0.25$). In comparison with the use of all initial input features, higher accuracy was found for the use of the 100% and 50% thresholds. The receiver operating characteristic (ROC) curve for the classification using the 100% threshold value is presented in Figure 1a. The classification accuracy for one test set – consisting of P4 and P7 – was below average ($M_{acc} = 44.00\%$). Further analysis showed that the incorrect classification was mainly relate to P4, where the wrong operation side was predicted for all cycles. For the remaining test sets, the classification accuracy was between 87.00% and 100.00% ($M_{acc} = 95.80 \pm 4.58\%$).

The occurrence of the ten highest ranked features of every fold is presented in Figure 1b. Overall, ten features occurred in the top ten rankings in ten out of the eleven folds (from HIP_ANGLE_X_54 to HF_a_80). The feature HIP_ANGLE_X_54 occurred in every fold in the top ten rankings. The correlations of those features are presented in Figure 1c. High to very high correlations were present (mean correlation = 0.63 ± 0.23).

Table 2. Model performance as mean accuracy (M_{acc}) and mean area under the curve (M_{AUC}) for the different approaches evaluated during leave-one-group-out cross-validation (LOGO). The 100% threshold refers to the use of all selected features. The true positives and true negatives are highlighted with a gray background color in the confusion matrix (CM). Similarity is reported as the mean Jaccard similarity (M_{Jacc}): 0 = no similarity, 1 = completely similar

Threshold	n feature	RF				mRMR					
		Macc [%]	MAUC	MJacc	CM	Macc [%]	MAUC	MJacc	CM		
1%	3.00 ±	87.36 ±	0.87 ±	0.64 ±	474	76	77.36 ±	0.79 ±	0.21 ±	456	94
	0.00	0.20	0.26	0.31	63	487	25.51	0.31	0.13	155	395
5%	15.82 ±	83.27 ±	0.82 ±	0.78 ±	453	97	76.73 ±	0.83 ±	0.23 ±	397	153
	0.40	24.27	0.36	0.24	87	463	25.80	0.30	0.08	103	447
10%	31.91 ±	83.82 ±	0.87 ±	0.78 ±	428	122	86.27 ±	0.89 ±	0.34 ±	461	89
	0.54	22.34	0.25	0.13	56	494	16.73	0.28	0.06	62	488
20%	64.55 ±	85.55 ±	0.90 ±	0.84 ±	446	104	88.73 ±	0.92 ±	0.46 ±	492	58
	1.13	18.83	0.19	0.06	55	495	15.55	0.21	0.05	66	484
50%	162.36 ±	89.55 ±	0.91 ±	0.85 ±	494	56	90.73 ±	0.92 ±	0.61 ±	512	38
	2.98	15.02	0.22	0.04	59	491	15.57	0.23	0.04	64	486
100%	325.45 ±	91.09 ±	0.91 ±	0.87 ±	511	39					
	5.04	16.28	0.25	0.02	59	491					
All initial features	8383	88.55 ±	0.91 ±	–	486	64					
		18.13	0.25		62	488					

The rankings of all features selected by RF with the mRMR filter are presented in Figure 1d. The ten highest ranked features showed little correlation (mean correlation = 0.35 ± 0.34). Using the mRMR ranking for classification with the different thresholds resulted in lower classification performance compared to that of the RF approach for the 1% and 5% thresholds. For the 10%, 20%, and 50% thresholds, the classification performance increased.

The gait waveforms of the highest ranked features and the selected discriminative time points are shown in Figure 2. Different gait patterns are prevalent for the operated and non-operated sides. Highly overlapping areas are noticeable.

Dimensionality reduction

The results for the different dimensionality reduction techniques are presented in Figure 3. Only slightly higher accuracy compared to the use of all initial input features could be reached by using LDA after applying PCA ($M_{acc} = 89.00 \pm 15.85\%$, $M_{AUC} = 0.93 \pm 0.18$).

Discussion

The current study demonstrates that the data-driven determination of parameters, which are most important for the description of asymmetrical gait in patients after THA, is possible. The basis for this is the classification of

THA patients according to the operation side. The operated side was predicted with high accuracy (91.09%) using the features selected with the proposed approach and a linear SVC. A higher accuracy was obtained compared to modeling with all initial input features (88.55%). The elimination of noisy, meaningless, and redundant variables could be a reason for the difference, which underlines the quality of the selected predictors. Using different classification algorithms (SVC with an rbf kernel, logistic regression) also leads to good classification results. Biases towards a specific classification algorithm were, therefore, low, which highlights the generalizability of the selected features.

Using 325.45 ± 5.04 features led to the best classification results. However, for practical applications, it should be decided if a less complex model could be sufficient. The use of only a few input variables could be especially beneficial for easier interpretation and, therefore, enhance the relevance in clinical contexts. In this regard, the results show that 87.36% of all cycles could be correctly classified with only three features.

Then, the predominantly occurring features in the top ten rankings were interpreted and validated using domain knowledge. Due to the initial centering of the marker position data, the direct interpretation through a comparison between the operated and non-operated sides for the marker-position-based features PSIS_Z_97, PSIS_Z_96, and ASIS_Z_14 is misleading.

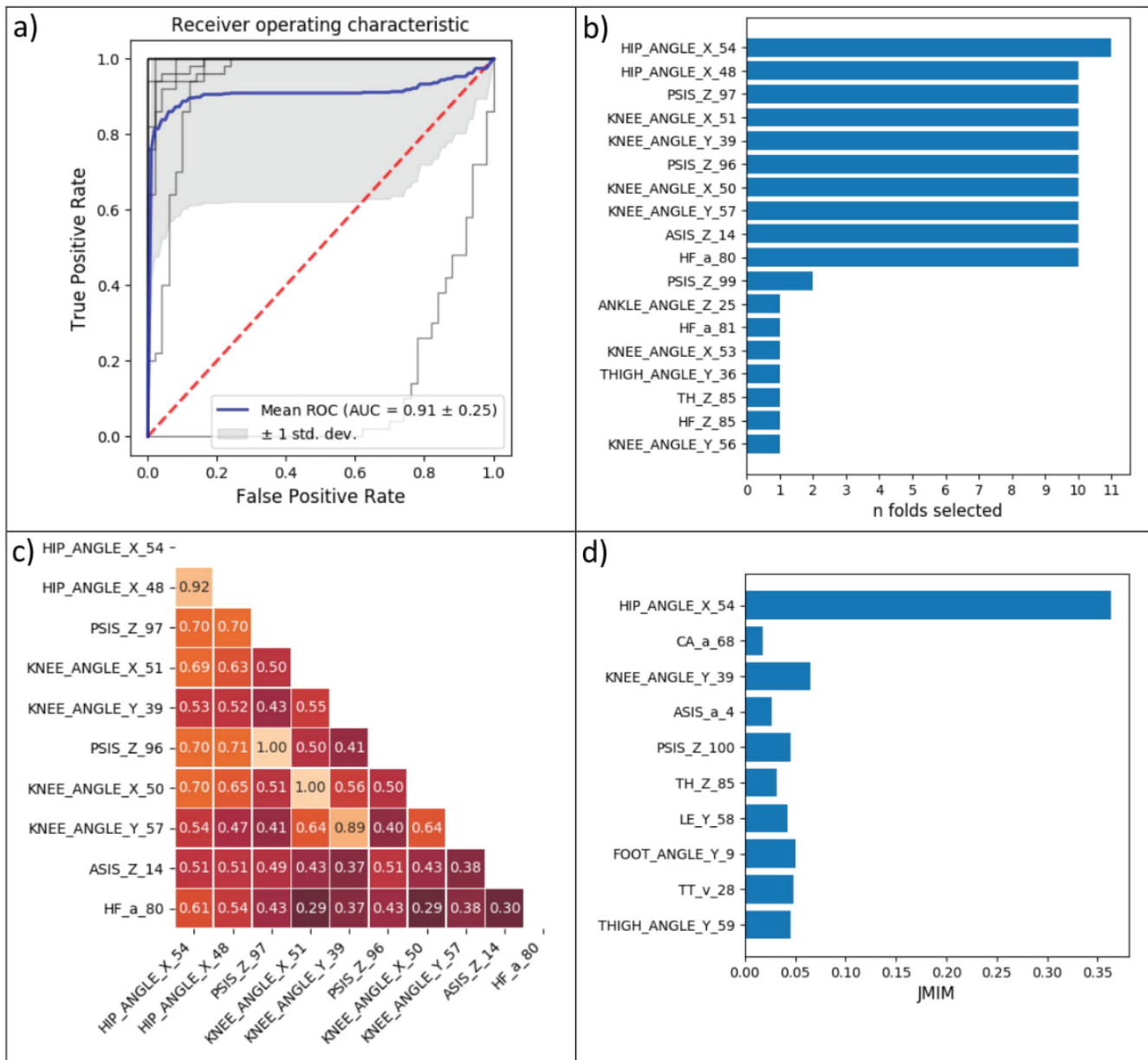


Figure 1. a) Receiver operating characteristic for each fold (gray lines) and for the mean (blue line). b) Numbers of times that features occurred in the top ten rankings of the LOGO folds (eleven folds in total). c) Correlation head map of the ten most stable features selected. d) Ranking of all selected features with the minimum-redundancy maximum-relevance filter, starting with the highest ranked feature at the top. The respective joint mutual information maximization (JMIM) scores [4] are plotted on the x-axis. Labelling: for the features representing joint and segment angles, X refers to movement in sagittal plane, Y to movement in frontal plane, and Z to movement in transverse plane

HIP_ANGLE_X_54 and HIP_ANGLE_X_48 highlight the importance of hip movement in the sagittal plane. HIP_ANGLE_X_54 was selected in the top ten rankings of every fold, and was also ranked as the feature with the highest relevance by the mRMR algorithm, which additionally highlights the discriminative power of the feature. Indirectly, due to the reduction of the minimal value for hip flexion/extension, a lower range of motion is relevant for classification. The effect has also been mentioned in previous studies [11, 29].

KNEE_ANGLE_X_51 and KNEE_ANGLE_X_50 represent knee movement in the sagittal plane. The knee shows increased flexion during the late stance phase. The predictors KNEE_ANGLE_Y_39 and KNEE_ANGLE_Y_57 show that, for class discrimination, knee abduction and adduction are important (movement in frontal plane). An altered varus has been reported in the literature [11]. The data revealed a bilateral valgus (abduction) for most patients, which was significantly increased for the operated side. A possible reason for the lateral difference

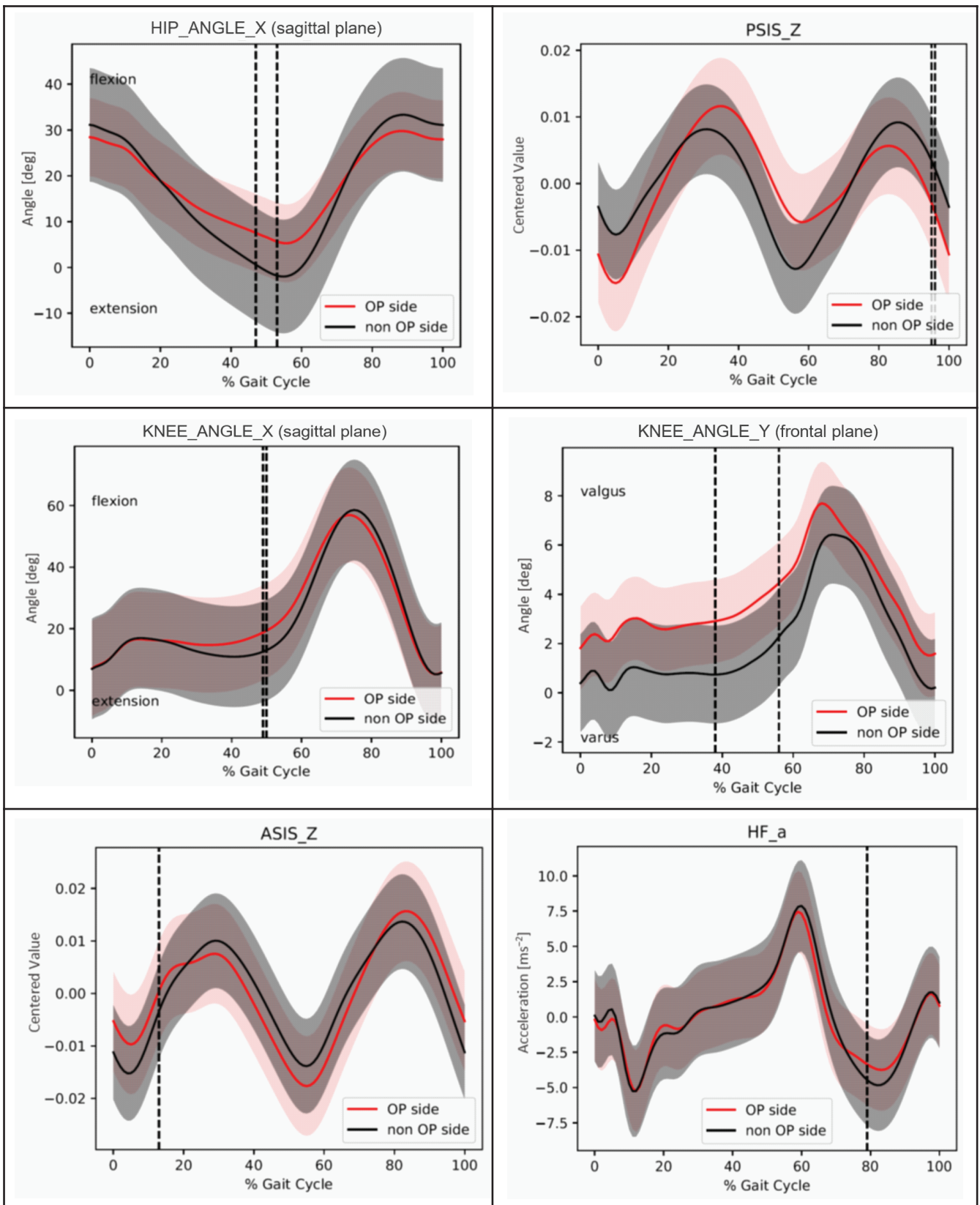


Figure 2. Asymmetric gait patterns (mean and standard deviation) in total hip arthroplasty (THA) patients. The points in time marked with a vertical line represent the most stable and highest ranked features. Note: Marker position data are centered

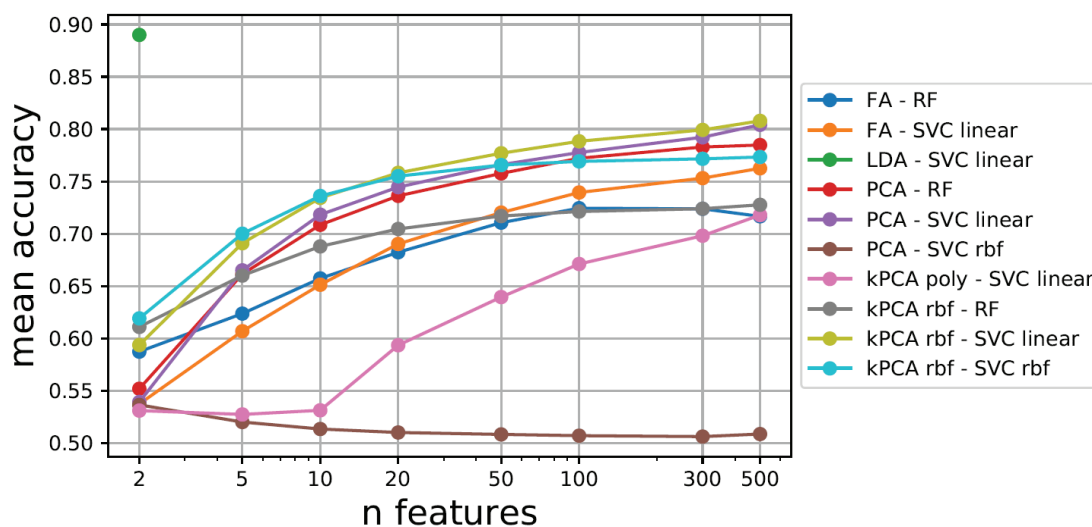


Figure 3. Model performance after dimensionality reduction; comparison of different techniques and different numbers of input features. Algorithms: FA = factor analysis, LDA = linear discriminant analysis, PCA = principal component analysis, kPCA = kernel PCA, RF = random forest, SVC = support vector classifier; kernels: poly = polynomial, rbf = radial basis function

is the reduced hip muscle strength on the operated side [31]. Furthermore, a general limitation of postoperative gait analysis is the potential influence of an abnormal pre-operative status, which has to be kept in mind as a possible bias. Moreover, the use of optical markers depends on the experience of the investigator and is therefore not free of errors when being placed on the anatomical landmarks through palpation [18]. Therefore, future studies should aim to verify these results with a higher sample size. Looking at feature HF_a_80, altered acceleration for the operated side is noticeable. Detailed biomechanical backgrounds for the marker-position – and acceleration-based features are not present and should be evaluated in the future. The rankings with the proposed RF approach as well as the rankings with the mRMR algorithm indicate that not only classical features, like joint angles, but also alternatives, like marker-position – or acceleration-data-based features, carry large amounts of information and show discriminative power.

The consideration above focuses on average characteristics, but individual patterns sometimes diverge (e.g., increased varus in patient 15). In line with the work of Chopra and Kaufman [11], the current study indicates a high variability in gait patterns (also see standard deviation) and possible subject-related differences and adaptations in patients after THA. Furthermore, the results for the single-subject analysis show that for P4, the wrong side was predicted as the operated side. The single-case analysis for P4 points out that when several variables were used as input features, altered inverted gait characteristics (e.g., for HIP_ANGLE_X and KNEE_ANGLE_Y) were prevalent compared to those of the remaining subjects. Therefore,

application of the classification algorithm could also be useful in identifying and individually addressing abnormal gait patterns in groups of patients after THA.

Several investigations demonstrated the potential of dimensionality reduction before gait classification [13, 14, 19]. In the present case, the combination of PCA and LDA showed similar classification results compared to the use of all initial inputs. The other methods applied showed considerably lower performance. However, compared to dimensionality reduction, better results were obtained with feature selection. Another advantage of the selection approach is that features can be immediately interpreted. The interpretation of principal components would require an additional interpretation step to analyze the components themselves. Nevertheless, dimensionality reduction allows the determination of dependencies between different parameters [30], which may be additionally relevant in clinical contexts. If only classification is important, application of the present combination of PCA and LDA seems especially promising because it is independent of a specification of a number of features to use.

Limitations arise from each patient wearing his or her own shoes instead of walking barefoot during gait analysis. It was shown, that different types of shoes influence the gait [33] and therefore introduce a bias during gait analysis. Moreover, placement of markers on the shoes instead of anatomical landmarks as well as relative motion of the shoes in respect to the feet might have influenced the study. Barefoot gait analysis should be considered for future analysis. To further evaluate the results, future research should also focus on a replication using different and increased numbers of subjects. The additional use of

kinetic data, as well as consideration of the sex – due to sex-specific differences in gait recovery after THA [15] – should also be analyzed. High variability in gait patterns and highly overlapping areas between the groups for the determined predictors may be limiting factors for accuracy. The development of an optimal experimental design that better maps group differences may be useful for increasing classification performance. With the use of waveforms as a starting point for feature selection, promising results could be obtained. However, further feature engineering could be profitable for an improvement of performance and should, therefore, be evaluated in future works.

Conclusions

The aim of the study was to find out, without relying on gait-specific assumptions or prior knowledge, which parameters are most important for the description of asymmetrical gait in patients after THA. In order to do this, meaningful features for classification of the side of the body that received a hip replacement were extracted from gait waveform data using a data-driven approach. The proposed RF approach seems promising for finding relevant features and their corresponding time points on the basis of high-dimensionality waveform data. This might be useful in identifying and individually addressing abnormal gait patterns during the rehabilitation process. For the present THA patients, the importance of features that represent hip movement in the sagittal plane and knee kinematics in the frontal and sagittal planes is emphasized. The use of marker position data of the anterior and posterior superior iliac spine, as well as acceleration data for markers placed at the proximal end of the fibula, is of further importance. The results indicate that studies should not only focus on variables like joint and segment angles because position and acceleration data also provide significant information.

Ethics Statement: The study was conducted according to the guidelines of the Declaration of Helsinki and approved by the Ethics Committee of Universität Paderborn. Informed consent was obtained from all subjects involved in the study.

Conflict of interest: Authors state no conflict of interest.

References

1. Afef B.B., Limam M. (2018) Ensemble feature selection for high dimensional data: a new method and a comparative study. *Adv. Data Anal. Classif.* 12(4): 937–952.
2. Beaulieu M.L., Lamontagne M., Beaulé P.E. (2010) Lower limb biomechanics during gait do not return to normal following total hip arthroplasty. *Gait & Posture* 32(2): 269–273.
3. Begg R., Kamruzzaman J. (2005) A machine learning approach for automated recognition of movement patterns using basic, kinetic and kinematic gait data. *J. Biomech.*, 38(3): 401–408.
4. Bennasar M., Hicks Y., Setchi R. (2015) Feature selection using Joint Mutual Information Maximisation. *Expert Syst. Appl.*, 42(22): 8520–8532.
5. Breiman L. (2001) Random Forests. *Machine Learning* 45: 5–32.
6. Bzdok D., Altman N., Krzywinski M. (2018) Statistics versus machine learning. *Nature Methods* 15(4): 233–234.
7. Cannas L.M., Dessì N., Pes B. (2013) Assessing similarity of feature selection techniques in high-dimensional domains. *Pattern Recognit. Lett.*, 34(12): 1446–1453.
8. Cappozzo A., Catani F., Della Croce U., Leardini A. (1995) Position and orientation in space of bones during movement: anatomical frame definition and determination. *Clin. J. Biomech.*, (Bristol, Avon) 10(4): 171–178.
9. Carse B., Meadows B., Bowers R., Rowe P. (2013) Affordable clinical gait analysis: an assessment of the marker tracking accuracy of a new low-cost optical 3D motion analysis system. *Physiother.*, 99(4): 347–351.
10. Chan H., Yang M., Wang H., Zheng H., McClean S., Sterritt R., Mayagoitia R.E. (2013) Assessing Gait Patterns of Healthy Adults Climbing Stairs Employing Machine Learning Techniques. *Int. J. Intell. Syst.*, 28(3): 257–270.
11. Chopra S., Kaufman K.R. (2018) Effects of Total Hip Arthroplasty on Gait. In: Müller B. and Wolf S. (eds.) *Handbook of Human Motion*, Springer, Cham, pp. 1–15. DOI: 10.1007/978-3-319-30808-1_81-1.
12. Dindorf C., Teuff W., Taetz B., Bleser G., Fröhlich M. (2020) Interpretability of Input Representations for Gait Classification in Patients after Total Hip Arthroplasty. *Sensors*, 20: 16.
13. Eskofier B.M., Federolf P., Kugler P.F., Nigg B.M. (2013) Marker-based classification of young-elderly gait pattern differences via direct PCA feature extraction and SVMs. *Comput. Methods Biomech. Biomed. Engin.*, 16(4): 435–442.
14. Figueiredo J., Santos C.P., Moreno J.C. (2018) Automatic recognition of gait patterns in human motor disorders using machine learning: A review. *Med. Eng. Phys.*, 53: 1–12.
15. Foucher K.C. (2016) Gait abnormalities before and after total hip arthroplasty differ in men and women. *J. Biomech.*, 49(14): 3582–3586.
16. Głowiński S., Łosiński K., Kowiański P., Waśkow M., Bryndal A., Grochulska A. (2020) Inertial Sensors as a Tool for Diagnosing Discopathy Lumbosacral Pathologic Gait: A Preliminary Research. *Diagnostics*, (Basel, Switzerland) 10(6): 342.

17. Horstmann, T., Listringhaus, R., Haase, G.-B., Grau, S., Mündermann, A. (2013) Changes in gait patterns and muscle activity following total hip arthroplasty: A six-month follow-up. *Clinical biomechanics (Bristol, Avon)* 28, 7: 762–769.
18. Hutchinson L., Schwartz J.B., Morton A.M., Davis I.S., Deluzio K.J., Rainbow M.J. (2018) Operator Bias Errors Are Reduced Using Standing Marker Alignment Device for Repeated Visit Studies. *J. Biomech. Eng.*, 140(4).
19. Ilias S., Tahir N.M., Jailani R., Hasan C.Z.C. (2017) Linear Discriminant Analysis in Classifying Walking Gait of Autistic Children. In: *2017 European Modelling Symposium (EMS)*. IEEE, pp. 67–72. DOI: 10.1109/EMS.2017.22.
20. Kalousis A., Prados J., Hilario M. (2007) Stability of feature selection algorithms: a study on high-dimensional spaces. *Knowl. Inf. Syst.*, 12(1): 95–116.
21. Kleemann R.U., Heller M.O., Stoeckle U., Taylor W.R., Duda G.N. (2003) THA loading arising from increased femoral anteversion and offset may lead to critical cement stresses. *J. Orthop. Res.*, 21(5): 767–774.
22. Laroche D., Tolambiya A., Morisset C., Maillefert J.F., French R.M., Ornetti P., Thomas E. (2014) A classification study of kinematic gait trajectories in hip osteoarthritis. *Comput. Biol. Med.*, 55: 42–48.
23. Leardini A., Sawacha Z., Paolini G., Ingrosso S., Nativio R., Benedetti M.G. (2007) A new anatomically based protocol for gait analysis in children. *Gait & Posture* 26(4): 560–571.
24. Liu F.T., Ting K.M., Zhou Z.-H. (2012) Isolation-Based Anomaly Detection. *ACM Trans. Knowl. Discov. Data*, 6(1): 1–39.
25. Liu H., Yu L. (2005) Toward Integrating Feature Selection Algorithms for Classification and Clustering. *IEEE Transactions on Knowledge and Data Engineering* 17(4): 491–502.
26. OECD. (2016) *Health at a Glance: Europe 2016. State of Health in the EU Cycle*. OECD Publishing, Paris.
27. Pedregosa F., Varoquaux G., Gramfort A., Michel V., Thirion B., Grisel O., Blondel M., Prettenhofer P., Weiss R., Dubourg V., Vanderplas J., Passos A., Cournapeau D. (2011) Scikit-learn: Machine Learning in Python. *J. Mach. Learn. Res.*, 12: 2825–2830.
28. Peng H., Long F., Ding C. (2005) Feature Selection Based on Mutual Information: Criteria of Max-Dependency, Max-Relevance, and Min-Redundancy. *IEEE Transactions on Pattern Analysis and Machine Intelligence*, 27(8): 1226–1238.
29. Perron M., Malouin F., Moffet H., McFadyen B.J. (2000) Three-dimensional gait analysis in women with a total hiparthroplasty. *Clin. Biomech.*, (Bristol, Avon), 15(7): 504–515.
30. Phinyomark A., Petri G., Ibáñez-Marcelo E., Osis S.T., Ferber R. (2018) Analysis of Big Data in Gait Biomechanics: Current Trends and Future Directions. *J. Med. Biol. Eng.*, 38(2): 244–260.
31. Rasch A., Dalén N., Berg H.E. (2010) Muscle strength, gait, and balance in 20 patients with hip osteoarthritis followed for 2 years after THA. *Acta Orthop.*, 81(2): 183–188.
32. Seijo-Pardo B., Bolón-Canedo V., Alonso-Betanzos A. (2019) On developing an automatic threshold applied to feature selection ensembles. *Inf. Fusion*, 45: 227–245.
33. Shakoor N., Sengupta M., Foucher K.C., Wimmer M.A., Fogg L.F., Block J.A. (2010) Effects of common footwear on joint loading in osteoarthritis of the knee. *Arthritis Care Res.*, 62(7): 917–923.
34. Teuffl W., Taetz B., Miezal M., Lorenz M., Pietschmann J., Jöllenbeck T., Fröhlich M., Bleser G. (2019) Towards an Inertial Sensor-Based Wearable Feedback System for Patients after Total Hip Arthroplasty: Validity and Applicability for Gait Classification with Gait Kinematics-Based Features. *Sensors*, 19(22): 5006.
35. Thewlis D., Bishop C., Daniell N., Paul G. (2013) Next-Generation Low-Cost Motion Capture Systems Can Provide Comparable Spatial Accuracy to High-End Systems. *J. Appl. Biomech.*, 29: 112–117.
36. Wang Z., Bao H.-W., Hou J.-Z. (2019) Direct anterior versus lateral approaches for clinical outcomes after total hip arthroplasty: a meta-analysis. *J. Orthop. Surg. Res.*, 14(1): 1–11.
37. Wong T.-T. (2015) Performance evaluation of classification algorithms by k-fold and leave-one-out cross validation. *Pattern Recognit.*, 48(9): 2839–2846.

Received 22.02.2021

Accepted 16.04.2021

© University of Physical Education, Warsaw, Poland

Acknowledgments

This research was funded by Offene Digitalisierungsallianz Pfalz, BMBF [03IHS075B].

We would like to thank the staff of the Klinik Lindenplatz, Bad Sassendorf, Germany for their support concerning the subject and data acquisition. We would especially like to thank Juliane Pietschmann and Thomas Jöllenbeck, who supported us with the recruitment and measurements.